Self-trapping problem of electrons or excitons in one dimension

G. Wellein and H. Fehske
Physikalisches Institut, Universität Bayreuth, D-95440 Bayreuth, Germany
(Received 19 December 1997; revised manuscript received 10 March 1998)

We present a detailed numerical study of the one-dimensional Holstein model with a view to understanding the self-trapping process of electrons or excitons in crystals with short-range particle-lattice interactions. Applying a very efficient variational Lanczos method, we are able to analyze the ground-state properties of the system in the weak- and strong-coupling, adiabatic and nonadiabatic regimes on lattices large enough to eliminate finite-size effects. In particular, we obtain the complete phase diagram and comment on the existence of a critical length for self-trapping in finite (closed) one-dimensional systems. In order to characterize large and small polaron states we calculate self-consistently the lattice distortions and the particle-phonon correlation functions. In the strong-coupling case, two distinct types of small polaron states are shown to be possible according to the relative importance of static displacement field and dynamic polaron effects. Special emphasis is on the intermediate-coupling regime, which we also study by means of direct diagonalization, preserving the full dynamics and quantum nature of phonons. The crossover from large to small polarons shows up in a strong decrease of the kinetic energy accompanied by a substantial change in the optical absorption spectra. We show that our numerical results in all important limiting cases reveal excellent agreement with both analytical perturbation theory predictions and very recent density matrix renormalization group data.
[S0163-1829(98)02034-7]

I. INTRODUCTION

Electrons, holes, or excitons delocalized in a perfect rigid lattice can be ''trapped'' within a potential well produced by displacements of atoms from their carrier-free equilibrium positions, provided the particle-lattice interaction is sufficiently strong.[1–4] Trapping of a carrier in this manner is more advantageous energetically as compared to wideband Bloch states, if the lowering of the carrier's energy due to its binding exceeds the strain energy required to produce the trap. Since the potential that binds the carrier depends on the carrier's state itself—i.e., the local distortion of the lattice is self-induced by the particle—this process is called ''self-trapping'' or ''autolocalization.'' Obviously, self-trapping (ST) is a highly nonlinear phenomenon. A self-trapped state is referred to as ''large'' if it extends over multiple lattice sites. Alternatively, if the quasiparticle is practically confined to a single site, the ST state is designated as ''small.'' Nonetheless, ST does not imply a breaking of translational invariance. ST eigenstates in a crystal are Bloch-like. Thus coherent transport of ST particles can, in principle, occur but the width of the corresponding band is extremely small (cf. the discussion in Ref. 5).

Introducing the concept of polarons into physics, the possibility of electron immobilization or ST was pointed out by Landau as early as 1933.[6] Shortly after, the ST of excitons was also suggested and studied theoretically.[7,8] ST polarons and excitons can be found in a wide variety of alkali metal halides, alkaline earth halides, II-IV and group IV semiconductors, condensed rare gases, organic molecular crystals, electrochromics, and other systems.[3,9] With the observation of polaronic effects in new materials exhibiting exceptional properties such as the high-T_c cuprates[10] or the colossal magnetoresistance manganates,[11] research on polarons has attracted renewed attention.

Although the problems of exciton and electron ST have much in common, there are fundamental differences. Most notably excitons are short-living nonequilibrium quasiparticles being immediately, after the optical excitation, in a free state and can reach the ST state only by tunneling through the potential barrier at low temperatures. Moreover, if the electron and hole, forming the exciton, have very different effective masses, the internal coordinates of this large-radius (Wannier-Mott) exciton will be of importance.

It is clear that the microscopic structure of the ST state is very diverse in various groups of materials. The stability of different types of ST states depends on the nature of the electron- or exciton-phonon (EP) coupling (e.g., deformation potential[12] against Fröhlich[13] coupling), the vibrational frequencies (e.g., acoustic vs optic), the dimensionality (D) of the lattice, and other parameters. A detailed classification of ST states and ST criteria is presented, e.g., in the excellent review of Rashba.[2] In particular, from a scaling treatment of a continuum lattice model in the adiabatic limit, it has been shown that in *multidimensional* systems ($D>1$) with only a *short-range nonpolar* EP interaction a ST carrier always forms a small polaron.[14,15,4] If there is an energy barrier that separates delocalized and spatial confined states, the free and ST states can coexist,[16,17] as evidenced, e.g., for solid xenon, by the coexistence of two exciton luminescence bands (one narrow and the other broad).[3] On the other hand, the presence of a *long-range polar* EP coupling ensures that at least the formation of large polaron states with moderate lattice deformation becomes possible. The picture is qualitatively changed when turning to *low-dimensional* systems. Recently it was shown that, unlike the continuum limit, the formation of a ST state in the two-dimensional (2D) case within a model of local EP coupling is always accompanied by the formation of an energy barrier attributed to the lattice discreteness.[18] The 1D case is essentially different from the

2D and 3D ones. In 1D ST proceeds without overcoming a barrier. To be more precise, the ST state is the ground state of the infinite system at any value of the EP coupling. In the weak-EP-coupling regime its radius exceeds several times the lattice spacing; i.e., a large polaron is formed even under the nonpolar interaction condition.[2]

Although the basic concepts underlying the ST transition are long standing and the gross features of ''large'' and ''small'' polarons and excitons have been extensively studied, our understanding of the ST problem is still incomplete. In particular the physically most important crossover regime, characterized by *intermediate*-EP-coupling strengths and phonon frequencies, is difficult to handle theoretically due to the failure of the standard phase transition concept.[19,20] As yet, there exist no well-controlled analytical techniques to describe the transition region. Other problems, for example, concern the existence of a critical length for ST in spatially restricted 1D systems,[21] the behavior of the polaron kinetic energy,[22] or the spectrum of light excitons under ST conditions.[2]

With these motivations, in this paper we want to discuss the ST problem using numerical methods. The focus is on the Holstein model in one dimension. By exact diagonalization of finite systems we analyze various ground-state and spectral properties of the model. Since for the Holstein model exact results are very rare[20,23,24] and previous numerical studies have been limited either to small systems or to a particular parameter regime,[25–29] this is a challenge by itself. Besides, we hope to gain more insight into the physics of small and large polarons and into the nature of the localization-delocalization transition.

The paper is organized as follows: In the next section we briefly introduce the Holstein model and outline our variational Lanczos approach that allows us to study the ground-state properties for all regimes of parameters on large lattices in a very efficient way. The numerical results will be presented in Sec. III. More precisely, the phase diagram of the Holstein model (Sec. III A), the electron lattice correlations (Sec. III B), the optical response (Sec. III C), and the kinetic energy (Sec. III D) will be discussed. The principal results are summarized in Sec. IV.

II. MODEL AND METHODS

With our focus on the self-trapping phenomenon in systems with only short-range nonpolar electron- or exciton-lattice interaction, it is appropriate to consider a model where a single excess carrier is placed in a one-dimensional periodic array of identical molecular units, each having an internal vibrational degree of freedom. Introducing electron (exciton) $a_i^{[\dagger]}$ and phonon $b_i^{[\dagger]}$ destruction [creation] operators we can write Holsteins's molecular crystal model[12] in lattice site representation as

$$\mathcal{H}=\hbar\omega_0\sum_i\left(b_i^\dagger b_i+\frac{1}{2}\right)-\sqrt{\varepsilon_p\hbar\omega_0}\sum_i(b_i^\dagger+b_i)n_i$$

$$-t\sum_{\langle ij\rangle}(a_i^\dagger a_j+a_j^\dagger a_i) \tag{1}$$

($n_i=a_i^\dagger a_i$; below $\hbar=1$). In the case of electrons the Holstein Hamiltonian (1) has been studied extensively as a paradigmatic model for small polaron formation. Here t denotes the nearest-neighbor free-electron transfer amplitude, ε_p is the strong-coupling polaron binding energy (in the atomic limit $t=0$), and ω_0 is the bare phonon frequency of the dispersionsless optical phonon mode. Referring to excitons we have in mind the small-radius (Frenkel or charge transfer) excitons only, and neglect, in the lowest order of approximation, the internal structure of the exciton: i.e., we consider it as a single neutral particle.

Generally speaking, the ground-state and spectral properties of the model (1) are governed by three ratios (control parameters) defined from the bare energy scales t, ω_0, and ε_p. First the adiabaticity parameter

$$\alpha=\omega_0/t \tag{2}$$

determines which of the two subsystems, excitons and electrons or phonons, is the fast and which is the slow one. In the adiabatic limit $\alpha\ll1$, the motion of the particle is affected by quasistatic lattice deformations (adiabatic potential surface) depending on the strength of the particle-phonon interaction. On the contrary, in the antiadiabatic limit $\alpha\gg1$, the lattice deformation is presumed to adjust instantaneously to the position of the carrier. Conveniently the particle is referred to as a ''light'' or ''heavy'' electron and exciton in the adiabatic or nonadiabatic regimes.[2] The second parameter is the dimensionless EP coupling constant

$$\lambda=\varepsilon_p/W, \tag{3}$$

where $W=2Dt$ denotes the half-width of the electron (exciton) band in a rigid D-dimensional lattice. Let us stress that λ represents the ratio between ''localization'' energy ($\propto\varepsilon_p$) and *bare* kinetic energy (W) of a single particle. Both λ and α are commonly used as parameters within a perturbative analysis of the Holstein model in the limits of weak ($\lambda\ll1$) and strong ($\lambda\gg1$) EP couplings. In the latter case two different approaches, based on expansions in powers of ($\alpha\ll1$) and ($1/\lambda\ll1$), have been elaborated for the adiabatic[12,16] and nonadiabatic[30] regimes, respectively. A third parameter

$$g^2=\varepsilon_p/\omega_0 \tag{4}$$

will be shown to be crucial in the strong-coupling situation. g^2 determines the relative deformation of the lattice which surrounds the particle.

In the limit of small particle density, a crossover between essentially delocalized carriers and quasilocalized particles is known to occur from early quantum Monte Carlo calculations,[31] provided that the *two* conditions $\lambda\gtrsim1$ and $g\gtrsim1$ are fulfilled. So while the first condition is more restrictive if α is small, i.e., in the adiabatic case, the formation of a small ST state will be determined by the second criterion in the antiadiabatic regime.[29,32,33]

It is not surprising that standard perturbative techniques are less able to describe the system close to the crossover region, where the energy scales are not well separated ($\lambda\sim1$, $g\sim1$). Therefore we will apply in the following two distinct numerical methods that allow investigating the ST phenomenon on finite clusters with great accuracy.

The *first method* is a variational Lanczos technique (developed originally for the Holstein t-J model[28,34]), which

enables us to study the *ground-state properties* of fairly large systems. In recent work this technique has been adapted successfully to treat the lattice degrees of freedom in the generalized double-exchange Hamiltonian commonly used for the description of colossal magnetoresistance materials.[35] In the case of the pure Holstein model, as a first step, we perform an inhomogeneous variational Lang-Firsov (IVLF) transformation

$$\tilde{\mathcal{H}}=\mathcal{U}^{\dagger}\mathcal{H}\mathcal{U}, \quad \mathcal{U}=e^{-\mathcal{S}_1(\Delta_i)}e^{-\mathcal{S}_2(\gamma)}e^{-\mathcal{S}_3(\tau)}, \tag{5}$$

with

$$\mathcal{S}_1(\Delta_i)=-\frac{1}{2g\alpha}\sum_i \Delta_i(b_i^{\dagger}-b_i), \tag{6}$$

$$\mathcal{S}_2(\gamma)=-\gamma g\sum_i (b_i^{\dagger}-b_i)a_i^{\dagger}a_i, \tag{7}$$

$$\mathcal{S}_3(\tau)=-\ln \tau^{-1/2}\sum_i (b_i^{\dagger}b_i^{\dagger}-b_i b_i) \tag{8}$$

(rescaling $\mathcal{H}=\mathcal{H}/t$ and measuring, in what follows, all energies in units of t). In a certain sense the canonical transformation $\mathcal{U}$ is a (variational) synthesis of two different approaches developed in the adiabatic[6,36,12,16] and antiadiabatic[7,8,37] theories of ST polarons and excitons. $\mathcal{S}_1$ introduces a set of static site-dependent displacement fields Δ_i related to local lattice distortions. This transformation ensures the correct behavior in the adiabatic limit. That is, $\mathcal{S}_1$ describes the ST of ''light'' excitons and electrons under the conditions that (i) the electronic bandwidth significantly exceed the characteristic phonon frequency and (ii) the lattice deformation energy be large (which allows one to treat the lattice vibrations quasiclassically). Within polaron theory such a type of ST quasiparticle is often called an adiabatic Holstein polaron.[12] $\mathcal{S}_2$, on the other hand, describes the ST process in the antiadiabatic limit. The variational parameter γ (with $0\leqslant\gamma\leqslant 1$) is introduced as a measure of the nonadiabatic phonon dressing of ''heavy'' particles, designated as ''localized'' excitons[38] or nonadiabatic Lang-Firsov small polarons. For $\gamma=1$, the well-known Lang-Firsov displaced-oscillator transformation results. In addition, we have applied the two-phonon squeezing transformation $\mathcal{S}_3$ $(0\leqslant\tau\leqslant 1)$.[39,40] The squeezing phenomenon is a many-particle effect, being of special importance at intermediate-EP-coupling strengths. This effect can be seen as a phonon frequency softening and tends to offset the (polaron) band narrowing. As a second step, we approximate the eigenstates $|\tilde{\Psi}\rangle$ of $\tilde{\mathcal{H}}$ by the variational states

$$|\tilde{\Psi}_V\rangle=|\tilde{\Psi}_{ph}\rangle\otimes|\tilde{\Psi}_{el}\rangle. \tag{9}$$

Then, performing in a third step the average over the transformed phonon vacuum, $\bar{\mathcal{H}}\equiv\langle\tilde{\Psi}_{ph}^0|\tilde{\mathcal{H}}|\tilde{\Psi}_{ph}^0\rangle$, we obtain the effective (electronic-excitonic) Hamiltonian

$$\bar{\mathcal{H}}=\frac{\alpha}{4}(\tau^2+\tau^{-2})N+\frac{1}{8\lambda}\sum_i \Delta_i^2-(1-\gamma)\sum_i \Delta_i n_i - 2\lambda\gamma(2-\gamma)\sum_i n_i - e^{-g^2\gamma^2\tau^2}\sum_{\langle ij\rangle}(a_i^{\dagger}a_j+a_j^{\dagger}a_i). \tag{10}$$

In Eq. (10), the first term leads to an increase of the zero-point energy of the phonons if $\tau^2<1$. The second and third contributions give the elastic energy and the particle-lattice interaction, respectively, both owing to the static lattice deformation. As a result of the incomplete LF transformation we get a constant (polaronic) level shift and an exponential band renormalization (fourth and fifth terms). Even the simplified model (10) cannot be solved exactly. Therefore we carry out a Lanczos diagonalization on finite N-site lattices using periodic boundary conditions (PBC's). Employing the Hellmann-Feynman theorem, the $N+2$ variational parameters can be obtained by iteratively solving the following set of self-consistency equations:

$$\Delta_i=4\lambda(1-\gamma)\bar{n}_i, \tag{11}$$

$$\gamma=\frac{\alpha[1-\bar{E}_{\Delta n}/4\lambda]}{\alpha-\tau^2 e^{-g^2\gamma^2\tau^2}\bar{E}_{kin}}, \tag{12}$$

$$\tau^2=\frac{\alpha}{\sqrt{\alpha^2-8\lambda\gamma^2 e^{-g^2\gamma^2\tau^2}\bar{E}_{kin}/N}}, \tag{13}$$

where

$$\bar{n}_i=\langle n_i\rangle_{\bar{\mathcal{H}}} \quad \text{with} \quad \sum_i \bar{n}_i=1, \tag{14}$$

$$\bar{E}_{kin}=-\sum_{\langle ij\rangle}\langle(a_i^{\dagger}a_j+a_j^{\dagger}a_i)\rangle_{\bar{\mathcal{H}}}, \tag{15}$$

$$\bar{E}_{\Delta n}=\sum_i \langle\Delta_i n_i\rangle_{\bar{\mathcal{H}}} \tag{16}$$

denote the local particle density, the kinetic energy, and the EP interaction contribution to the ground-state energy, respectively. Note that each iteration step involves the exact diagonalization of $\bar{\mathcal{H}}(\gamma,\tau^2,\{\Delta_i\})$. We note further that the Hamiltonian (10) potentially contains symmetry-broken states which originate from inhomogeneous displacement fields $\Delta_i\neq 0$. Therefore we have to work with an unsymmetrized set of basis states.

The *second method* we are going to use in the computational work is the direct numerical diagonalization of the initial Holstein Hamiltonian (1). On the one hand, this should bring out valuable information on the applicability of various approximative analytical and numerical approaches. In particular we would like to test the quality of IVLF-Lanczos scheme described so far. On the other hand, combining our exact diagonalization (ED) algorithm with the Chebyshev recursion and maximum entropy methods,[41] we are able to discuss the *dynamical properties* of the systems, e.g., the optical conductivity, in more detail. Moreover, ED provides

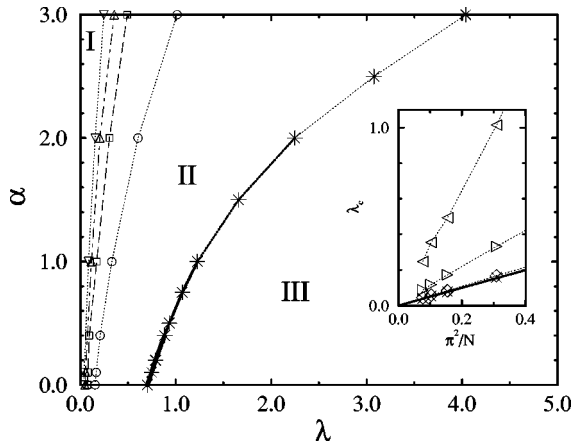

FIG. 1. Phase diagram of the 1D Holstein model. Nearly free polarons, large polarons, and small polarons exist in the regions I, II, and III, respectively. Results are obtained for finite rings with $N=32$ (○), 64 (□, ∗), 96 (△), and 128 (▽) sites using the IVLF-Lanczos method. The inset shows the critical coupling for self-trapping, λ_c, at $\alpha=0$ (×), 0.1 (◇), 1.0 (▷), and 3.0 (◁). The solid line gives the relation (17). For further explanation see the text.

the only reliable tool for treating the transition regime. Differently from the IVLF-Lanczos treatment the translational invariance of the system is ensured. The ED method, based on a well-controlled truncation procedure of the phonon Hilbert space, has been described elsewhere.[42,32,33,43] Using parallel computers, we are able to diagonalize systems with a total dimension of 10^{10}.

III. NUMERICAL RESULTS AND DISCUSSION

A. Phase diagram

In the numerical work we start with a discussion of the ground-state properties of the transformed Hamiltonian (10). Applying the IVLF-Lanczos technique presented in the previous section, we have determined the phase diagram of the 1D Holstein model. The results are depicted in Fig. 1. First let us consider regimes II and III, corresponding to large and small polarons, respectively. Just for brevity we will use in the following the ''polaron terminology,'' keeping in mind that all statements hold for the case of Frenkel excitons as well. The distinct types of polarons, found in regimes II and III, may be characterized by the spatial extension and strength of the (inhomogeneous) lattice displacements Δ_i and by the magnitude of the polaron variational parameter γ (see below). From *exact* analytical[20] and numerical[31,42,29] (cf. also Sec. III D) results it is well known that the large-size polaron turns *continuously* into a small-size polaron with increasing EP coupling. Since there is no true phase transition between large and small ST states at $\alpha>0$, the transition line (stars) shown in Fig. 1 only indicates the crossover region, which gets wider as the phonon frequency (α) increases. Within our IVLF-Lanczos treatment, the transition line has been fixed by the criterion $\Delta_1/\Delta_0=1/e$. Performing a finite-size analysis of the II⇌III transition, we found that the results obtained for the 64-site lattice almost agree with the extrapolated values for the infinite system. Via Eq. (11), Δ_i is directly related to the polaron density at site i. Of course, this condition can only give a crude estimate of the ''transition'' from large to small polarons, in particular in the nonadiabatic regime where the static Δ_i are less significant. According to the importance of the Δ_i ($\alpha\leqslant 1$) and γ ($\alpha\geqslant 1$) effects, the small polaron formed in region III will be called an adiabatic Holstein polaron (AHP) and nonadiabatic Lang-Firsov polaron (NLFP), respectively.

As a peculiarity of our *finite* system with PBC's a further strongly finite-size dependent transition to a nearly-free-electron state (phase I) is observed by lowering the EP coupling strength. In other words, it seems that a critical coupling $\lambda_c(N)$ or equivalently a critical system size $N_c(\lambda)$ exists for self-trapping in 1D. Indeed, for the 1D *continuum model*, where the ST problem can be described by a nonlinear Schrödinger equation, it has been shown recently by Rashba[21] that the ST condition is

$$\lambda>\lambda_c=\pi^2/2N. \tag{17}$$

This relation holds rigorously within the adiabatic theory[21] and is reproduced by our *lattice model* calculation as well (cf. inset Fig. 1). At $\alpha=0$, the nearly free-electron phase (phase I) corresponds to a solution with $\gamma=0$ and $\Delta_i=\Delta=4\lambda/N$. The kinetic energy, however, is unrenormalized.

Our IVLF-Lanczos scheme allows us to extend the above considerations to the finite-phonon-frequency regime. Again, at low EP couplings, we found a nearly-free-electron phase with a small uniform level shift ($\propto -2\lambda[\gamma(2-\gamma)+2(1-\gamma)^2/N]$). More significantly, since we have $\gamma>0$ now, the inclusion of nonadiabatic phonon effects slightly renormalizes the electron half-bandwidth $\bar{W}=2\exp\{-g^2\gamma^2\tau^2\}$. If λ becomes larger than $\lambda_c(\alpha)$, the ST proceeds by a monotonic lowering of the total energy without overcoming a ST barrier. This is in accordance with the expansion of the total energy of the continuum model near the ST threshold in the adiabatic limit $\alpha\to 0$, which yields a smooth behavior of $E_0(\lambda)$ with a discontinuity only in the second derivative.[21] The scaling of $\lambda_c(\alpha)$ with N is shown in the inset of Fig. 1. At λ_c a minimum in the total energy develops, which corresponds to a state with inhomogeneous lattice deformations. For a discrete lattice model with PBC's it is a formidable task to analyze analytically the ground-state energy profile as a function of a multidimensional lattice deformation coordinate $Q=\{\Delta_i\}$. This is because the shape of the energy functional is determined by the complicated interplay of kinetic and (confinement-strain) potential energy contributions. However, the existence of a critical system size for self-trapping may be understood easily from the fact that the (noninteracting) electron spectrum exhibits finite-size gaps [due to the discrete set of the N allowed Bloch ($\vec{K}$) levels]. Consequently, to gain energy by forming a large-size (wave-packet) ST state the system has to overcome at least the lowest of these gaps by EP coupling effects. Then, as a feedback effect, the electronic band structure itself is weakly renormalized by the electron-lattice interaction. In the thermodynamic limit $N\to\infty$ the finite-size gaps vanish, and we obtain $\lambda_c(\alpha)\to 0$. Thus, in an *infinite* 1D (ring) system self-trapping takes place at any finite value of the EP coupling. Moreover, let us anticipate that $\lambda_c=0$ holds also for *finite* 1D Holstein systems with *open boundary conditions* (see Sec. III B).

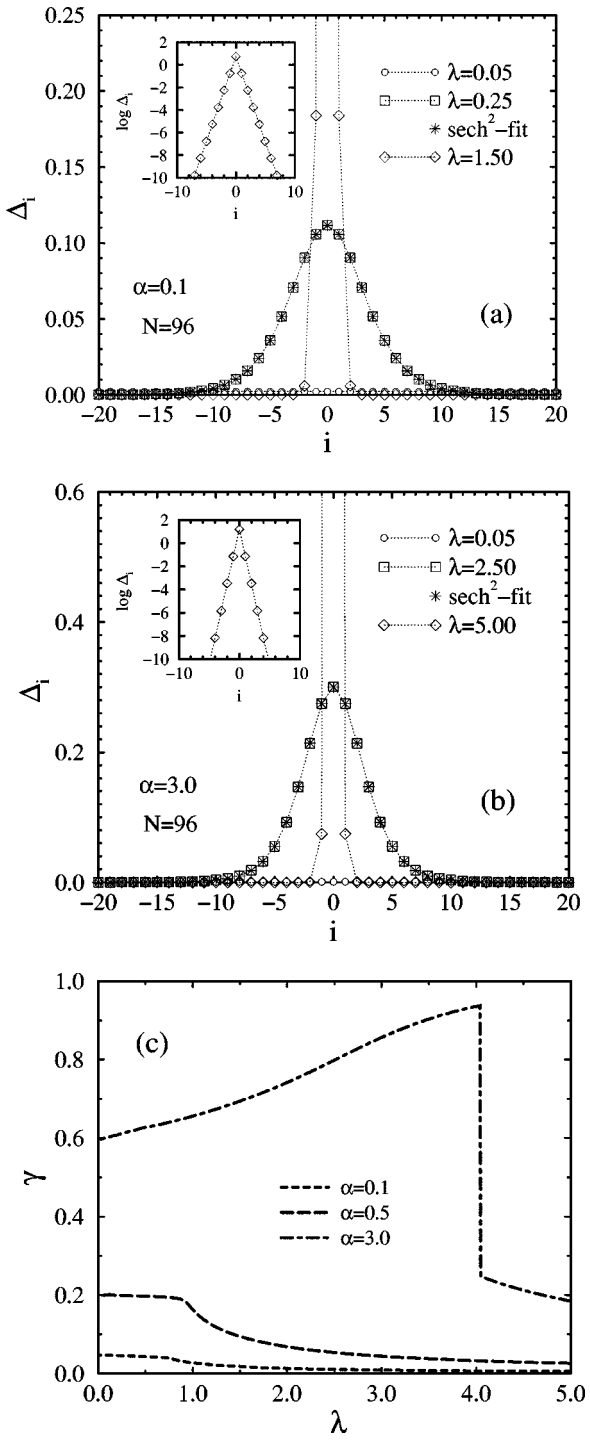

FIG. 2. Variation of the displacement fields Δ_i away from the central site 0 for several characteristic EP couplings λ in the adiabatic (a) and nonadiabatic (b) regimes. The dependence of the Lang-Firsov polaron variational parameter γ on λ is depicted in (c).

To elucidate in more detail the different nature of polaronic states occurring in the ground-state phase diagram of the effective model (10), we present in Fig. 2 the behavior of the variational parameters.

First of all, we should emphasize that, studying the *single-electron* problem, the squeezing effect ($\tau^2<1$) is only of minor importance. This is obvious from Eq. (13), which yields $\tau^2=1$ in the thermodynamic limit. For finite systems, the leading $(1/N)$ corrections ($\propto g^2\gamma^2 e^{-g^2\gamma^2\tau^2}\overline{E}_{kin}/\alpha N$) tend to zero in the weak- and strong-coupling adiabatic and antiadiabatic limits.

The spatial extension of the static lattice deformation (Δ_i) is visualized in Figs. 2(a) and 2(b) for different EP couplings corresponding to the nearly free, large and small polaron cases. As discussed above, the Δ_i are being constant for $\lambda<\lambda_c(\alpha)$ (phase I). For the large-size polaron (phase II), the lattice displacements fit extremely well to the relation

$$\Delta_i=\Delta_0\,\mathrm{sech}^2[\lambda_{eff}i], \tag{18}$$

where $\lim_{\alpha\to 0}\lambda_{eff}(\lambda,\alpha)=\lambda$. It is worth emphasizing that the functional form (18), which has been derived in the framework of an adiabatic continuum theory,[16,44,18] also describes the displacement fields in the nonadiabatic large-polaron regime. Obviously, λ_{eff} defines a characteristic inverse length scale in the system; i.e., the radius of the large polaron is approximately given by $(2\lambda_{eff})^{-1}$. For $\alpha=0.1$ and $\lambda=0.25$ we obtained $\lambda_{eff}/\lambda\simeq 0.935$. On the other hand, at $\alpha=3$ and $\lambda=2.5$, the effective coupling becomes strongly reduced: $\lambda_{eff}/\lambda\simeq 0.116$. In the strong-coupling regime, we observe an exponential decay $\Delta_i\simeq\Delta_0 e^{-i/\xi}$ of the lattice distortion away from the polaron site (see insets), where ξ denotes the small-polaron radius. We found $\xi\simeq 0.29$ (0.19) for $\lambda=1.5$ (5.0) and $\alpha=0.1$ (3.0); i.e., in both cases the ST state is mainly confined to a single lattice site. While in the framework of our interpolating theory the Δ_i can be taken as a measure of the ''adiabatic character'' of the polaronic quasiparticle, its ''nonadiabatic part'' is described by the Lang-Firsov variational parameter γ shown in Fig. 2(c). Of course, in the case of ''light'' electrons ($\alpha<1$), the nonadiabatic polaron effect is rather small. In particular for $\lambda>1$, when the small AHP is formed, γ becomes strongly suppressed. Here the renormalization of the polaron band is mainly driven by the static displacement fields Δ_i. Otherwise, for ''heavy'' electrons, we observe larger values of γ, which increase with increasing EP coupling strength. As a result the free-electron band is transformed into a renormalized polaron band. Due to the (generalized) Franck-Condon factor $e^{-g^2\gamma^2\tau^2}$, the bandwidth is exponentially small under strong-coupling conditions (g^2, $\lambda\gg 1$), where also the K-dependent corrections to the band dispersion become negligible.[33] Within our variational approach we found a first-order transition to the AHP state at an extremely strong EP interaction ($\lambda_{II/III}\simeq 4$, for $\alpha=3$). However, this sharp transition is in some sense an artifact of our IVLF scheme that compares the ground-state energies of the AHP and NLFP states, both obtained in the lowest order of approximation [remember that by deriving Eq. (10) we have performed the average over the *zero-phonon* state only]. Including higher-order corrections, the NLFP with $\gamma\to 1$ is stabilized in the nonadiabatic strong-coupling regime (cf. the discussion in Sec. III D).

As stated at the beginning of this section, we have tried to explore the phase diagram of the Holstein model and the nature of the ST transition by calculating various ground-state properties of the system under consideration. An alternative method was used in recent numerical work by Kopidakis *et al.*[45] (see also Vekhter and Ratner[46]), who solved the (time-dependent) discrete nonlinear Schrödinger equation for

a single tight-binding electron coupled to *acousticlike* (anharmonic[46]) eigenvibrations, where the lattice degrees of freedom are treated *classically*. The results of this semiclassical approach depend very strongly on the initial electronic configuration. When the initial energy of the electron is close to the bottom of the band, i.e., in the vicinity of the pure electronic ground state, the main characteristics of polaron formation, discussed above for the adiabatic and nonadiabatic cases, were obtained. On the other hand, for an initially highly excited electron, the ST is much more complex, and, in general, the tendency towards electron localization is reduced as the initial energies get higher. Here we are not in the position to check the quality of these results. Within an exact diagonalization approach the way to study excited states is to calculate, e.g., the single-particle spectral function. For the simple Holstein model this has be done by a number of authors quite recently.[22,33,47]

B. Electron-lattice correlations

In looking for a characterization of the different polaronic regimes for the *quantum-phonon* Holstein model (1), we have computed the (normalized) correlation function between the electron position $i=0$ and the oscillator displacement at site j,

$$\chi_{0,j}=\frac{\langle n_0(b_{0+j}^{\dagger}+b_{0+j})\rangle}{2g\langle n_0\rangle}, \tag{19}$$

by means of a direct diagonalization technique. Here fermion and boson degrees of freedom are related by the relation $\langle b_i^{\dagger}+b_i\rangle_{\mathcal{H}}=2g\langle n_i\rangle_{\mathcal{H}}$ ($=2g/N$ for the single-electron case).

Alternatively, working with the effective Hamiltonian (10), the electron-lattice correlation function (19) can be expressed as

$$\overline{\chi}_{0,j}=\gamma\delta_{0,j}+\frac{\Delta_j}{4\lambda}. \tag{20}$$

Hence we can use the static correlation functions $\chi_{0,j}$ and $\overline{\chi}_{0,j}$ to test the accuracy of the IVLF scheme.

Figure 3 shows the static correlation functions (19) and (20) in the adiabatic (a) and nonadiabatic (b) regimes for several coupling parameters λ corresponding to the different polaronic ''phases'' indicated in Fig. 1. For parameters close to the adiabatic weak-coupling regime (phase I), the amplitude of $\chi_{0,j}$ is extremely small and the spatial extent of the electron-induced lattice deformation is spread over the whole lattice. For correctness it should be stated that the nearly-free-electron phase I, stabilized by the kinetic energy contribution, only occurs in finite 1D Holstein systems with PBC's. If we apply open boundary conditions (OPC's) on a finite chain the electron density $\overline{n}_i$ is inhomogeneous even at $\lambda=0$. Thus, according to Eq. (11), we found a large-size polaron with spatially varying Δ_i for any $\lambda>0$. The corresponding electron-lattice correlations are depicted in Fig. 3(a) for open chains with $N=17$ sites (in order to get a symmetric solution about $j=0$). Needless to say that the PBC and OBC IVLF results coincide for $N\to\infty$.

In the quantum-phonon model (1) the coupling gives rise to a weak dressing of the electron at any finite α. However,

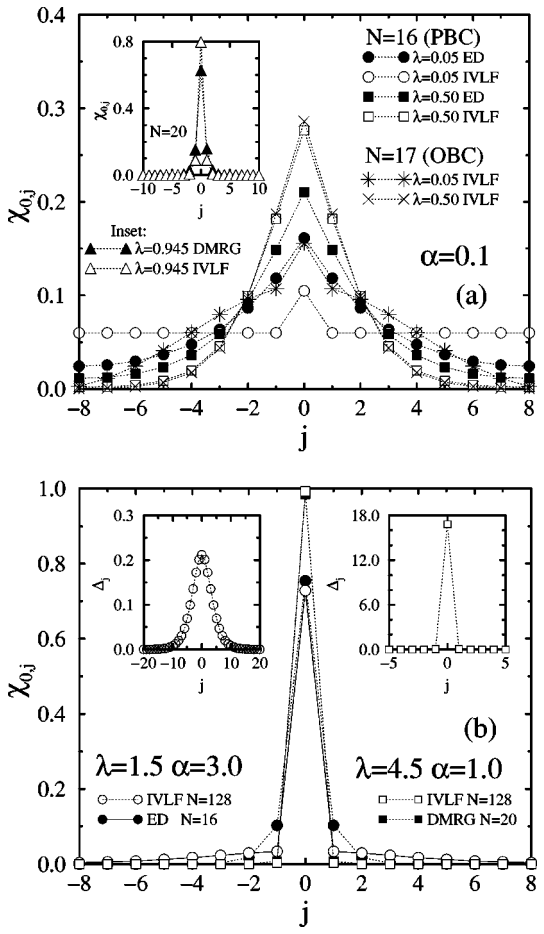

FIG. 3. Electron-lattice correlations $\chi_{0,j}$ in the adiabatic weak-to-intermediate EP coupling (a) and nonadiabatic intermediate-to-strong EP coupling (b) cases. IVLF-Lanczos results are compared with ED data and the DMRG results taken from Ref. 48. In (a), cross and star symbols denote the IVLF-Lanczos results obtained by using open boundary conditions (OBC's).

the carrier is not trapped due to the zero-point quantum lattice fluctuations.[48] From Eq. (20) it is clear that in the effective model (10) the on-site dynamical polaron and spatially extended static displacement field contributions are well separated. Neglecting the residual polaron-phonon interaction, the IVLF approach describes the real situation by a (variational) superposition of both effects. In the adiabatic large-polaron region II a much better description of the exact behavior is obtained. Especially when the small AHP state evolves at $\lambda\sim 1$ the IVLF results are even in quantitative agreement with the density matrix renormalization group (DMRG) data obtained very recently by Jeckelmann and White[48] [see inset Fig. 3(a)]. At this point we would like to emphasize that performing such DMRG and, in particular, ED calculations requires much more memory and CPU-time resources than our extreme simple and very fast IVLF computations. In Fig. 3, the system sizes treated within the IVLF scheme have been restricted in order to make possible a direct comparison with the available ED and DMRG data.

Obviously, for intermediate to strong EP couplings, the IVLF results agree almost exactly with the ED and DMRG data [Fig. 3(b)]. Here the electron-lattice correlations become very localized and finite-size and boundary-condition effects are less important. Although the behavior of $\chi_{0,j}$, shown in

the main part of Fig. 3, is found to be very similar for $\lambda = 1.5$, $\alpha = 3.0$ and $\lambda = 4.5$, $\alpha = 1.0$, we would like to emphasize that both parameter sets describe completely different physical situations. The distinct nature of the corresponding small-polaron states becomes apparent from the variation of the static displacement fields shown in the insets. For $\lambda = 4.5$ and an intermediate (or low) phonon frequency, we observe a static lattice distortion in the vicinity of the electron only. Since $\Delta_0/4\lambda \sim 1$, in Eq. (20), the second term dominates the first one and we obtain a small AHP confined to a single site. On the contrary, for $\lambda = 1.5$ and $\alpha = 3$, we are still in the large-polaron region II due to the high phonon frequency [cf. Fig. 1 and the spatial extension of the static lattice distortion shown in the left inset of Fig. 3(b)]. Nevertheless, the correlations between the electron and the phonon remain local. But now, since the $\Delta_j/4\lambda$ are small for all j, the peak structure of $\chi_{0,j}$ at $j = 0$ results from the first term in Eq. (20). That means it is mainly triggered by the γ effect ($\gamma \simeq 0.69$). This interpretation is substantiated by our ED results, yielding a mean phonon number in the ground state of about 0.625, which clearly indicates that the zero-phonon state is still the most probable one. Therefore the approximation we applied by deriving Eqs. (10) and (20) is justified.

C. Optical response

Extremely valuable information on the low-energy excitations in interacting electron- or exciton-phonon systems can be obtained by studying their optical response. Actually, the optical absorption of small polarons is distinguished from that of large (or quasifree) polarons by the shape and the temperature dependence of the absorption bands which arise from exciting the ST carrier from or within the potential well that binds it.[4] Furthermore, as was the case with the ground-state properties, the optical spectra of light and heavy electrons and excitons differ essentially as well.[2] In the most simple weak-coupling and nonadiabatic strong-coupling limits, the absorption associated with photoionization of Holstein polarons is well understood and the optical conductivity can be analyzed analytically[49–53] (for a detailed discussion of small-polaron transport phenomena we refer to the review of Firsov[54]). Serious problems, caused, for example, by the complicated behavior of the adiabatic potential surface, arise if one tries to calculate the spectrum of self-trapped light excitons.[2] Moreover, the intermediate-coupling and -frequency regime is as yet practically inaccessible for a rigorous analysis. On the other hand, previous numerical studies of the optical absorption in the Holstein model were limited to very small two- or four-site clusters.[27,29] In order to calculate the optical conductivity numerically in a wide parameter range on fairly large systems, we have implemented our computer code, which is based on a combination of Lanczos diagonalization, Chebyshev recursion, and maximum entropy methods,[41,43] on parallel machines.

The real part of the optical conductivity, $\mathrm{Re}\,\sigma(\omega) = \mathcal{D}\delta(\omega) + \sigma^{reg}(\omega)$, can be decomposed into the Drude weight δ function at $\omega = 0$ and a regular part ($\omega > 0$) written in spectral representation at $T = 0$ as[55]

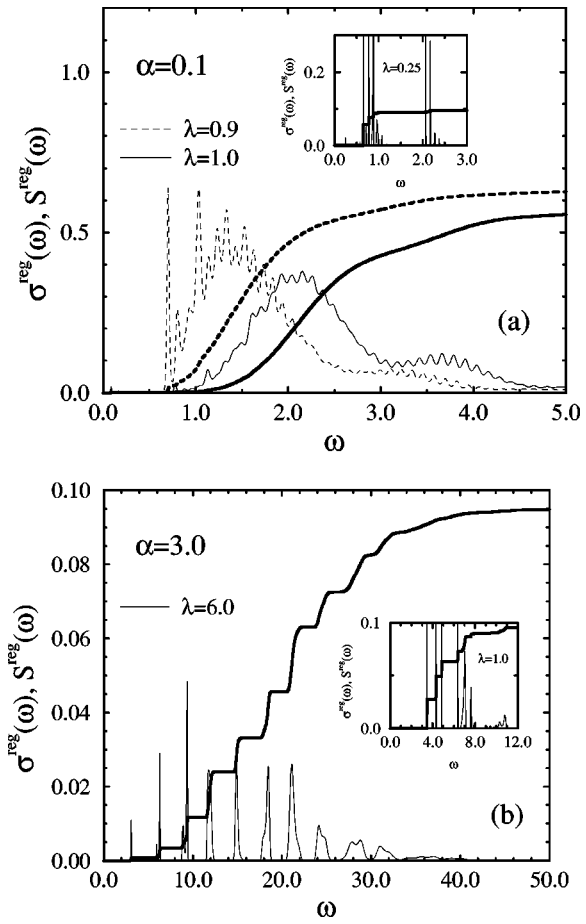

FIG. 4. Optical absorption in the 1D Holstein model. For $N = 8$ and $M = 25$, the regular part of the conductivity σ^{reg} (thin lines) and the integrated spectral weight S^{reg} (thick lines) are plotted as a function of ω at different EP couplings for the ''light'' (a) and ''heavy'' (b) electron cases.

$$\sigma^{reg}(\omega) = \sum_{m \neq 0} \frac{|\langle \Psi_0 | i\Sigma_j (a_j^\dagger a_{j+x} - a_{j+x}^\dagger a_j) | \Psi_m \rangle|^2}{E_m - E_0} \times \delta(\omega - E_m + E_0). \tag{21}$$

In Eq. (21), $\sigma^{reg}(\omega)$ is given in units of πe^2 and we have omitted the $1/N$ prefactor. For the discussion of the optical properties it is useful to consider the spectral weight function

$$\mathcal{S}^{reg}(\omega) = \int_0^\omega d\omega' \, \sigma^{reg}(\omega') \tag{22}$$

as well.

Numerical results for both $\sigma^{reg}(\omega)$ and $\mathcal{S}^{reg}(\omega)$ are presented in Fig. 4. We will start with the somewhat more subtle case of *light electrons*.

But first let us recall that, restricting ourselves to phononic states $|s\rangle_{ph} = \Pi_{i=0}^{N-1} (1/\sqrt{n_i^s!}) (b_i^\dagger)^{n_i^s} |0\rangle_{ph}$ with at most M phonons, a K-symmetrized state of the Holstein model is given as $|\Psi_K\rangle = \Sigma_{m=0}^{M} \Sigma_{s=1}^{\overline{S(m)}} c_K^{m,s} |K; m, \overline{s}\rangle$, where $\overline{S(m)} = (N-1+m)!/(N-1)!m!$ (for more details see Refs. 33,43). K denotes the *total* momentum of the coupled EP system. Then, if the EP coupling is finite, the ground state $|\Psi_0\rangle$ and all excited states $|\Psi_m\rangle$ contain components that

correspond to m-phonon states (with $m=\Sigma_{i=0}^{N-1} n_i^s \leqslant M$, $n_i^s \in [0,m]$) in the tensorial product Hilbert space of electronic and phononic states. When the EP coupling is small ($\lambda \ll 1$), these multiphonon states have less spectral weight; i.e., the phonon distribution of the ground state, $|c_0^m|^2(M) = \Sigma_s |c_{K=0}^{m,s}|^2$, exhibits a pronounced maximum at the zero-phonon state.[33] The maximum of $|c_0^m|^2(M)$ is shifted to larger values of m as λ increases.

Keeping this in mind and noticing further that in Eq. (21) an optical transition can take place only within the $K=0$ sector ($|\Psi_0\rangle \equiv |\Psi_{K=0}\rangle$), the peak structure of σ^{reg} shown in Fig. 4(a) may be easily understood in connection with the single-particle spectrum. For low phonon frequencies ($\alpha \ll W$), the energy to excite one phonon lies inside the bare tight-binding band $E_K^{(0)} = -2t \cos K$ and we observe a flattening of the coherent band structure E_K at large momenta.[32,56] Then the coherent bandwidth $\Delta E = E_\pi - E_0$ is approximately given by α ($\ll [E_K^{(0)} - E_0^{(0)}]$), i.e., by the phonon frequency, where the states at finite momenta are predominantly ''phononic'' states with less ''electronic'' spectral weight. Thus, although in principle an optical excitation can be achieved by ''adding'' phonons with opposite momentum to these states (in order to reach the $K=0$ sector), the overlap to the mainly ''electronic'' ground state is extremely small. Therefore we found, roughly speaking, the first transitions with non-negligible weight to the free-electron states and its vibrational satellites [see $S^{reg}(\omega)$]. This is perfectly illustrated by the inset of Fig. 4(a). Here the first and second groups of peaks are approximately located at the bare tight-binding energies $E_K^{(0)}$ ($+n\alpha$), for the allowed wave vectors of the eight-site lattice used in the numerical calculation ($K=\pi/4, \pi/2, \ldots$). Of course, with increasing the lattice size the K values will become dense and we will obtain the monotonous decay of the optical absorption coefficient observed for large polarons above the photoionization threshold.[4] To understand the changes in the optical absorption in the crossover region from a large-size polaron to small AHP, the main part of Fig. 4(a) shows σ^{reg} at two intermediate-EP-coupling parameters. In this case the coherent band structure E_K gets stronger renormalized, but more important, the phonon distribution function in the ground state, $|c_0^m|^2(M)$, becomes considerably broadened. For instance, at $\alpha=0.1$, we have $|c_0^m|^2(M=25) \simeq 0.008$ ($m=0$), 0.095 ($m=7$), and 0.008 ($m=18$) and $|c_0^m|^2(M=25) \simeq 0.0002$ ($m=0$), 0.1 ($m=12$), and 0.0005 ($m=24$) for $\lambda=0.9$ and $\lambda=1.0$, respectively. Therefore the overlap with excited multiphonon states is enlarged and the optical response is enhanced. The line shape of the absorption bands reflects the phonon distribution in the ground state, where the small oscillations are due to the discreteness of the phonon frequency. As a result, the peak structure is smeared out and the wide sidebands, belonging to different electronic momenta (e.g., $K=\pi/4$ and $K=\pi/2$), merge with each other.

We now turn to the *heavy electron* case [Fig. 4(b)]. The inset again illustrates the behavior in the large-polaron regime ($\lambda=1$, $\alpha=3$; cf. Fig. 1), where a rather moderate band renormalization occurs ($\Delta E \sim 2.33$ due to the flattening effect[32]). But now the phonon frequency is large compared to the finite-size gaps between the first mainly ''electronic'' excitations ($E_K - E_0 < \alpha$ for $K \leqslant \pi/2$). Therefore, in contrast to the light electron case [cf. Fig. 4(a)], the different absorption bands (each built up by several ''electronic'' K levels) can be classified according to the number of phonons involved in the optical transition. As can be seen from the main part of Fig. 4(b), the absorption spectrum for a small-size polaron is quite different from that of a large polaron. According to the results of Sec. III A, a small NLFP is formed in the strong-coupling nonadiabatic limit. Here the phonons will heavily dress the electron and, concomitantly, the ''electronic character'' of the resulting strongly renormalized small polaron band becomes suppressed (cf. the discussion of the K-dependent wave-function renormalization factor $\mathcal{Z}_K^{(a)} = |\langle \Psi_K | a_K^\dagger | \Psi_0 \rangle|^2$ in Ref. 33). For our parameters ($\lambda=6$, $g^2=4$), the maximum in the phonon distribution function is located between $m=3$ and 4. The renormalized bandwidth is small compared to all other energy scales ($\Delta E \sim 0.0782 \ll \alpha, 2W$). Since the current operator connects only states having a substantial overlap as far as the phononic state is concerned, multiphonon absorptions (i.e., nondiagonal transitions[50]) become now increasingly important in the optical response. This leads to the peak structure observed for the nonadiabatic small-polaron optical conductivity in Fig. 4(b). Obviously, the different bands are being separated by multiples of the bare phonon frequency. The height of the jumps in the ω-integrated conductivity is directly related to the probability of the corresponding absorption process. We found that substantial spectral weight stays in the lower-energy part of the spectrum at frequencies comparable to $\varepsilon_p = 2\lambda (\simeq m_{max}\alpha)$. These absorptions, resembling to some extent a large polaron's absorption, are signatures of a ST polaron with intermediate size. In the extreme strong-coupling limit the dominant absorption process results from the transfer of the ST carrier to the neighboring site without changing the lattice distortion. That means that the optical absorption spectrum should exhibit a single-peak structure at $\omega = 2\varepsilon_p = 4\lambda$, which corresponds to the lowering of the electronic energy associated with the small-polaron formation.[57,51] This feature already evolves for the coupling strength considered in Fig. 4(b) (cf. ΔS^{reg} for the seventh absorption band).

D. Kinetic energy

Further information about the transition from large to small polarons can be obtained from the behavior of the polaron kinetic energy E_{kin}. Replacing $\overline{\mathcal{H}}$ by $\mathcal{H}$, the kinetic energy can be easily obtained from the static correlation function (15). On the other hand, according to the f-sum rule, E_{kin} is directly related to the ω-integrated optical conductivity,

$$-\frac{E_{kin}}{2} = \mathcal{S}^{tot} = \frac{\mathcal{D}}{2\pi e^2} + \mathcal{S}^{reg}. \tag{23}$$

Calculating, via Eqs. (21) and (22), $\mathcal{S}^{reg} = \mathcal{S}^{reg}(\infty)$ numerically allows us to determine the Drude weight $\mathcal{D}$ as well. Sometimes one defines an effective polaronic transfer amplitude,[28,22] $t_{p,eff} = E_{kin}(\lambda)/E_{kin}(0)$, in order to characterize the polaron mobility. In our reduced units we have $t_{p,eff} \equiv \mathcal{S}^{tot}$. From Eq. (23) it is obvious that $t_{p,eff}$ includes both coherent and incoherent transport processes. Hence

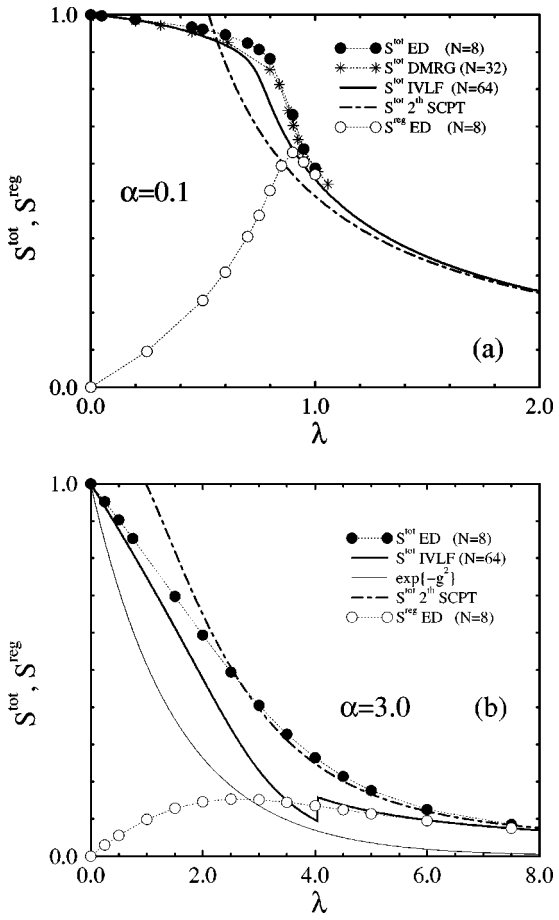

FIG. 5. Kinetic energy [in units of $(-W)$] S^{tot} and contribution of σ^{reg} to the f-sum rule, S^{reg}, as a function of the EP coupling λ in the adiabatic (a) and nonadiabatic (b) regimes. Circles (stars) denote exact [DMRG (Ref. 48)] data obtained for a lattice with $N=8$ (32) sites. IVLF-Lanczos results (solid curves) are compared with the predictions of standard first-order ($\bar{W}/W=\exp\{-g^2\}$, thin solid line) and second-order (chain-dashed curves) perturbation theory.

$t_{p,eff}$ substantially differs from the exponential factor e^{-g^2}, obtained in lowest-order perturbation theory, and cannot be used to determine the coherent bandwidth ΔE under strong-coupling conditions $(\lambda, g^2 \gg 1)$.

The evolution of the kinetic energy ($\mathcal{S}^{tot}$) as a function of the EP coupling λ is displayed in Figs. 5(a) and 5(b) for the case of light and heavy electrons, respectively. In agreement with previous numerical results,[31,28,22,48] E_{kin} clearly shows the crossover from a large polaron, characterized by a $\mathcal{S}^{tot}$ that is only weakly reduced from its noninteracting value $[\mathcal{S}^{tot}(\lambda=0)=1]$, to a less mobile small AHP (NLFP) in the adiabatic (nonadiabatic) strong-coupling limit.

For *low phonon frequencies* $[\alpha=0.1$, Fig. 5(a)], we found a rather narrow transition region. As recently pointed out by Capone *et al.*,[29] the decrease of $\mathcal{S}^{tot}$ in the crossover regime is driven by the sharp fall of the Drude weight. By contrast the optical absorption due to inelastic scattering processes, described by the regular part of the optical conductivity, becomes strongly enhanced[33] (see the behavior of $\mathcal{S}^{reg}$). It is worth emphasizing that the IVLF results for $\mathcal{S}^{tot}(\lambda)$ are in excellent agreement with the ED and DMRG data.

The large- to small-polaron transition is considerably broadened at *high phonon frequencies* $[\alpha=3.0$, Fig. 5(b)]. Here the IVLF results start to deviate from the exact ones when g^2 becomes much larger than 1, thus making the lowest-order zero-phonon approximation inherent in the IVLF scheme less justified. As mentioned already in Sec. III A, the nonanalytic jumplike behavior at $\lambda \sim 4$ is an apparent shortcoming of the variational approach which compares ground-state energies only.

Although for large enough g and λ the simple formula $\bar{W}=W\exp\{-g^2\}$, which should not be identified with the ''Lang-Firsov approach,'' [22,58] works perfectly well in the determination of the *coherent bandwidth* $(\Delta E \simeq 2\bar{W})$,[27,33] the need of going beyond the lowest order of approximation to obtain reliable results for the *kinetic energy* has been emphasized many times.[1,33,48,59,58] In the nonadiabatic strong-coupling limit $(g^2 \gg 1, \alpha > 1)$, the ground-state energy obtained within second-order perturbation theory is a tiny bit lower than the IVLF energy and almost coincides with the ED result. Adapting the second-order strong-coupling approach presented in our previous work[33] to the 1D case (with $\gamma=1$), the kinetic energy is obtained, via $E_{kin}^{SCPT}=t\partial_t\langle\mathcal{H}\rangle$, as

$$E_{kin}^{SCPT}=-\frac{4}{\alpha}\left\langle\frac{1}{s}\right\rangle_{\kappa=2g^2}-e^{-g^2}\left[2+\frac{4}{\alpha}\left\langle\frac{1}{s}\right\rangle_{\kappa=g^2}\right]. \quad (24)$$

Here $\langle\cdots\rangle_\kappa$ means the average with respect to the Poisson distribution with parameter κ. As can be seen from Fig. 5, at large EP interactions, strong-coupling perturbation theory (SCPT) gives a sufficiently accurate description of $\mathcal{S}^{tot}$ in both the adiabatic and nonadiabatic regimes.

IV. SUMMARY

The main objective of this study was to reexamine in detail the self-trapping transition of electrons and excitons in one dimension within the framework of the Holstein model by the use of computational techniques. The calculations are performed by exact diagonalizations of finite systems, where the full dynamics and quantum nature of phonons were taken into account. Therefore the results are unbiased and allow one to test the applicability of a numerically much more efficient variational Lanczos approach proposed by the authors. This IVLF-Lanczos technique is designed to analyze strongly correlated electron-phonon models on fairly large lattices, including static displacement field, nonadiabatic polaron, and squeezing effects. The comparison between IVLF results and ED data, performed in this paper, clearly shows that the simple IVLF-Lanczos approach provides an exceptional good description of the ground-state properties of the Holstein model, in particular for the light electron case.

Let us summarize the main outcome of our work.

Figure 6 illustrates the basic physics contained in the single-particle Holstein model. This model describes a continuous transition from large to small polarons with increasing EP coupling strength. Depending on the adiabaticity of the system, $\alpha=\omega_0/t$, the crossover regime is determined by the more stringent of the two conditions $\lambda=\varepsilon_p/2Dt \gtrsim 1$ and $g^2=\varepsilon_p/\omega_0 \gtrsim 1$. Thus starting from ''light'' $(\alpha<1)$ or ''heavy'' $(\alpha>1)$ electrons it is possible to understand the formation of small adiabatic ''Holstein'' or nonadiabatic

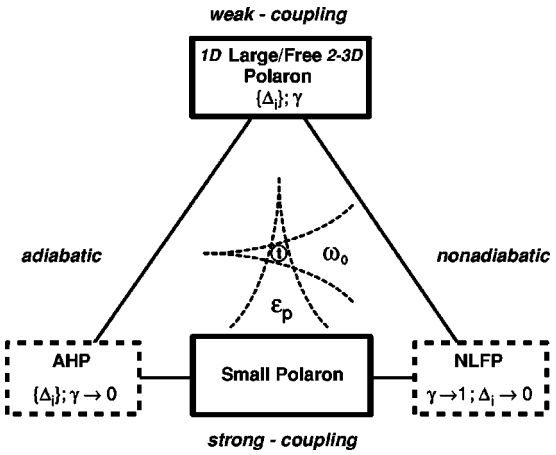

FIG. 6. Schematic phase diagram of the Holstein model.

''Lang-Firsov'' polarons as two limiting cases of a general picture.

In the infinite 1D Holstein model the self-trapped state is the ground state for any value of the EP coupling. As a specific property of a finite 1D Holstein system with periodic boundary conditions, a critical length or equivalently a critical EP coupling strength exists for self-trapping, rigorously at least at $\omega_0=0$.[21] This may be of importance for closed (spatially restricted) systems like C_{60}. By contrast, there is no critical length and coupling if the system has open ends, which is important for nanowires.

The large-size polaron is characterized by spatially extended lattice deformations. Within our IVLF description, the variation of the displacement fields follows the (adiabatic) formula $\Delta_i \propto \mathrm{sech}^2[\lambda_{eff} i]$ even in the nonadiabatic regime, but with a strongly reduced inverse length scale given by an effective coupling constant $\lambda_{eff}(\lambda,\alpha) \ll \lambda$. The mean phonon number in the large-polaron ground state is rather small. In 2D and 3D Holstein systems a large-polaron phase does not exist.

The small-polaron state is basically a multiphonon state characterized by strong on-site electron-phonon correlations. Due to a large local static lattice distortion, the AHP becomes quasilocalized on a single site. Also the NLFP is immobile because it has to drag with it a large number of phonons in its phonon cloud.

The intermediate-EP-coupling and -phonon-frequency regime is hardly accessible to traditional analytical methods, mainly because the kinetic and EP interaction (potential) energies, favoring a delocalization and localization of the charge carriers, respectively, are equally important. Here the residual polaron-phonon interaction generates further than nearest-neighbor ranged hopping processes and the resulting effective polaronic band dispersion deviates from a simple tight-binding cosine band (cf. the discussion in Ref. 32). The transition from large to small polarons is accompanied by significant changes in the single-particle spectral properties[33] as well as in the optical response of the system. In particular, for ''light'' electrons the spectral weight of the regular part of the optical conductivity is strongly enhanced at the transition. For ''heavy'' electrons the line shape of the optical absorption spectra is highly asymmetric in the intermediate-to-strong-coupling regime and therefore differs considerably from the usual small-polaron hopping behavior obtained for $g^2 \gg 1$.

As a result of self-trapping the mobility of the charge carriers is reduced. The behavior of the kinetic energy indicates that the crossover region from large to small ST states is rather narrow (broad) in the adiabatic (nonadiabatic) regimes. The formation of small adiabatic Holstein polarons is accompanied by a dramatic kinetic energy loss mainly driven by a sharp drop of the Drude weight. Since both the bandwidth and the (electronic) spectral weight of the small-polaron band are exponentially reduced in the extreme strong-coupling case $g^2, \lambda \gg 1$, coherent small-polaron transport becomes rapidly destroyed by thermal fluctuations.

In principle our ED approach allows a full quantum mechanical description of the dynamics, i.e., the time evolution, of coupled EP (Holstein) systems. Such an investigation would be highly desirable since first attempts to examine this problem,[45] which are based, however, on a classical treatment of the lattice, indicate a much greater complexity of the ST phenomenon if the electron subsystem is initially a highly excited configuration. Especially the temporal energy redistribution between the electronic and vibrational degrees of freedom, found in several EP models with optical[22] and acoustic-phonon-deformation potential[45,46] couplings, deserves further verification including the effects of quantum lattice dynamics. Work in this direction will be started in the near future.

ACKNOWLEDGMENTS

The authors would like to thank J. Loos and D. Ihle for many helpful discussions. We are greatly indebted to E. Jeckelmann and S. R. White for putting their DMRG data at our disposal. Special thanks go to the LRZ München, HLRZ Jülich, and the HLR Stuttgart for the generous granting of their computer facilities. This work was performed under the auspices of Deutsche Forschungsgemeinschaft, SFB 279.

[1] Y. A. Firsov, *Polarons* (Nauka, Moscow, 1975).

[2] E. I. Rashba, in *Excitons*, edited by E. I. Rashba and M. D. Sturge (North-Holland, Amsterdam 1982), p. 543.

[3] K. S. Song and R. T. Williams, *Self-Trapped Excitons* (Springer-Verlag, Berlin, 1993).

[4] D. Emin, in *Polarons and Bipolarons in High-T_c Superconductors and Related Materials*, edited by E. K. H. Salje, A. S. Alexandrov, and W. Y. Liang (Cambridge University Press, Cambridge, England, 1995).

[5] Y. Bar-Yam, T. Egami, J. M. de Leon, and A. R. Bishop, *Lattice Effects in High-T_c Superconductors* (World Scientific, Singapore, 1992).

[6] L. D. Landau, Z. Phys. **3**, 664 (1933).

[7] R. Peierls, Ann. Phys. (N.Y.) **13**, 905 (1932).

[8] J. Frenkel, Phys. Z. Sowjetunion **9**, 158 (1936).

[9] A. L. Shluger and A. M. Stoneham, J. Phys.: Condens. Matter **5**, 3049 (1993).

[10] E. K. H. Salje, A. S. Alexandrov, and W. Y. Liang, *Polarons and*

Bipolarons in High Temperature Superconductors and Related Materials (Cambridge University Press, Cambridge, England, 1995).
[11] A. J. Millis, P. B. Littlewood, and B. I. Shraiman, Phys. Rev. Lett. **74**, 5144 (1995).
[12] T. Holstein, Ann. Phys. (N.Y.) **8**, 325 (1959).
[13] H. Fröhlich, Adv. Phys. **3**, 325 (1954).
[14] Y. Toyozawa and A. Sumi, in *Proceedings of the XII International Conference on the Physics of Semiconductors*, edited by M. H. Pilkuhn (Teubner, Stuttgart, 1974).
[15] D. Emin and T. Holstein, Phys. Rev. Lett. **36**, 323 (1976).
[16] E. I. Rashba, Opt. Spektrosk. **2**, 78 (1957).
[17] Y. Toyozawa, Prog. Theor. Phys. **26**, 29 (1961).
[18] V. V. Kabanov and O. Y. Mashtakov, Phys. Rev. B **47**, 6060 (1993).
[19] B. Gerlach and H. Löwen, Phys. Rev. B **35**, 4291 (1987).
[20] H. Löwen, Phys. Rev. B **37**, 8661 (1988).
[21] E. I. Rashba, Synth. Met. **64**, 255 (1994).
[22] E. V. L. de Mello and J. Ranninger, Phys. Rev. B **55**, 14 872 (1997).
[23] J. K. Freericks and E. H. Lieb, Phys. Rev. B **51**, 2812 (1995).
[24] S. Ciuchi, F. de Pasquale, and D. Feinberg, Europhys. Lett. **30**, 151 (1995).
[25] J. Ranninger and U. Thibblin, Phys. Rev. B **45**, 7730 (1992).
[26] F. Marsiglio, Phys. Lett. A **180**, 280 (1993).
[27] A. S. Alexandrov, V. V. Kabanov, and D. K. Ray, Phys. Rev. B **49**, 9915 (1994).
[28] H. Fehske, H. Röder, G. Wellein, and A. Mistriotis, Phys. Rev. B **51**, 16 582 (1995).
[29] M. Capone, W. Stephan, and M. Grilli, Phys. Rev. B **56**, 4484 (1997).
[30] A. A. Gogolin, Phys. Status Solidi B **109**, 95 (1982).
[31] H. D. Raedt and A. Lagendijk, Phys. Rev. Lett. **49**, 1522 (1982).
[32] G. Wellein and H. Fehske, Phys. Rev. B **56**, 4513 (1997).
[33] H. Fehske, J. Loos, and G. Wellein, Z. Phys. B **104**, 619 (1997).
[34] H. Fehske, Habilitationsschrift, Universität Bayreuth, 1996.
[35] H. Röder, J. Zang, and A. R. Bishop, Phys. Rev. Lett. **76**, 1356 (1996).
[36] S. I. Pekar, Zh. Eksp. Teor. Fiz. **16**, 335 (1946).
[37] I. G. Lang and Y. A. Firsov, Zh. Eksp. Teor. Fiz. **43**, 1843 (1962) [Sov. Phys. JETP **16**, 1301 (1963)].
[38] A. S. Davydov, *Theory of Molecular Excitons* (McGraw-Hill, New York, 1962).
[39] H. Zheng, Solid State Commun. **65**, 731 (1988).
[40] D. Feinberg, S. Ciuchi, and F. de Pasquale, Int. J. Mod. Phys. B **4**, 1317 (1990).
[41] R. N. Silver, H. Röder, A. F. Voter, and J. D. Kress, J. Comput. Phys. **124**, 115 (1996).
[42] G. Wellein, H. Röder, and H. Fehske, Phys. Rev. B **53**, 9666 (1996).
[43] B. Bäuml, G. Wellein, and H. Fehske, Phys. Rev. B **58**, 3663 (1998).
[44] A. H. Castro Neto and A. O. Caldeira, Phys. Rev. B **46**, 8858 (1992).
[45] G. Kopidakis, C. M. Soukoulis, and E. N. Economou, Phys. Rev. B **51**, 15 038 (1995).
[46] B. G. Vekhter and M. A. Ratner, Phys. Rev. B **51**, 3469 (1995).
[47] J. M. Robin, Phys. Rev. B **56**, 13 634 (1997).
[48] E. Jeckelmann and S. R. White, Phys. Rev. B **57**, 6376 (1998).
[49] D. Emin, Phys. Rev. B **48**, 13 691 (1993).
[50] G. D. Mahan, *Many-Particle Physics* (Plenum Press, New York, 1990).
[51] H. G. Reik and D. Heese, J. Phys. Chem. Solids **28**, 581 (1967).
[52] J. Loos, Z. Phys. B **71**, 161 (1988).
[53] H. Fehske, D. Ihle, J. Loos, U. Trapper, and H. Büttner, Z. Phys. B **94**, 91 (1994).
[54] Y. A. Firsov, Semiconductors **29**, 515 (1995).
[55] E. Dagotto, Rev. Mod. Phys. **66**, 763 (1994).
[56] W. Stephan, Phys. Rev. B **54**, 8981 (1996).
[57] M. I. Klinger, Phys. Lett. **7**, 102 (1963).
[58] Y. A. Firsov and E. K. Kudinov, Fiz. Tverd. Tela **39**, 2159 (1997) [Phys. Solid State **32**, 1930 (1997)].
[59] A. S. Alexandrov and N. F. Mott, *Polarons and Bipolarons* (World Scientific, Singapore, 1995).